Reanalysis of Boron Adsorption on Soils and Soil Minerals Using the Constant Capacitance Model

Sabine Goldberg*

ABSTRACT

Inclusion of microscopic information improved the ability of the constant capacitance model to provide a quantitative description of B adsorption on various Al and Fe oxides, clay minerals, and arid-zone soils as a function of solution pH. The same set of B surface complexation reactions was used for all adsorbing surfaces. This study tests the ability of the model to describe B adsorption using surface configurations that had been observed experimentally. In the present model application, both trigonal, $B(OH)_3$, and tetrahedral, $B(OH)_4^-$, B surface complexes are postulated, consistent with experimental spectroscopic results. Boron surface complexation constants for Al and Fe oxides and kaolinites are not statistically significantly different from each other. Boron surface complexation constants for kaolinites are statistically significantly different from those for 2:1 clays and soils. Boron surface complexation constants for 2:1 clays and soils are not statistically significantly different from each other, reflecting the dominance of 2:1 clay minerals in B adsorption reactions in arid-zone soils. Average sets of B surface complexation constants provided adequate descriptions of B adsorption behavior on all adsorbents studied, indicating some predictive capability. The constant capacitance model was able to predict B adsorption behavior on additional arid-zone soils using the average set of B surface complexation constants.

BORON IS AN ESSENTIAL MICRONUTRIENT for plant growth. The range between deficiency and toxicity symptoms is narrow, necessitating accurate quantification of soil solution B concentrations (Reisenauer et al., 1973). Because plants respond only to solution B concentrations, adsorption reactions of B on soil minerals potentially attenuate phytotoxic soil solution concentrations. In arid areas, B toxicity results from additions via the irrigation water and from high levels of B in soils. In soil solution, 0.2 mg L^{-1} is considered deficient and 1 mg L^{-1} is considered toxic, determined as hot water–soluble B (Adriano, 1986).

Various modeling approaches have been used to describe B adsorption on soils and soil minerals. Historically, adsorption isotherm equations such as the Langmuir equation and the Freundlich equation provided descriptions of B adsorption on soil materials (e.g., Elrashidi and O'Connor, 1982; Goldberg and Forster, 1991). Adsorption isotherms are empirical models whose parameters are only valid for the particular conditions under which the experiment was conducted. More recently, various surface complexation models have been used to describe B adsorption on soils and soil minerals (Goldberg and Glaubig, 1985, 1986a, 1986b; Bloesch et al., 1987; Singh and Mattigod, 1992; Toner and Sparks, 1995). Surface complexation models are chemical models that define surface species, chemical reactions, mass balances, and charge balance. Surface complexation models contain molecular features that can be given thermodynamic significance (Sposito, 1983).

The constant capacitance model was developed to describe ion adsorption at the oxide–solution interface (Stumm et al., 1980) and has been used to describe B adsorption on oxides (Goldberg and Glaubig, 1985), clay minerals (Goldberg and Glaubig, 1986b), and soils (Goldberg and Glaubig, 1986a). Conventionally, surface complexation reactions for anion adsorption in the constant capacitance model are written in terms of undissociated acids (Stumm et al., 1980). The number of anion surface complexes considered is equal to the number of dissociations undergone by the acid. Because H_3BO_3 is a weak monobasic acid ($pK_a = 9.2$), Goldberg and Glaubig (1985, 1986a, 1986b) considered one B surface complex in their model descriptions of B adsorption. For Al and Fe oxides and kaolinite minerals, good fits of the model to the data were obtained by optimizing only the B surface complexation constant (Goldberg and Glaubig, 1985). To adequately describe B adsorption on the 2:1 clay minerals montmorillonite and illite and soil samples, it was necessary to optimize values for the protonation–dissociation constants along with that of the B surface complexation constant. Even so, chemically unrealistic values of the protonation–dissociation constants were obtained in some cases, reducing the chemical significance of the model application to a curve-fitting procedure (Goldberg and Glaubig, 1986a, 1986b).

Recent work by Su and Suarez (1995) has provided direct spectroscopic evidence for the presence of B in both trigonal, $B(OH)_3$, and tetrahedral, $B(OH)_4^-$, geometries on the surface of amorphous Fe oxide. The authors analyzed mineral pastes using Attenuated Total Reflectance Fourier Transform Infrared (ATR-FTIR) spectroscopy. Because water was present in the samples, the results of Su and Suarez (1995) are directly applicable to natural soil systems.

The objectives of the present study are: (i) to reevaluate the ability of the constant capacitance model to describe B adsorption on oxides, clay minerals, and soils including microscopic experimental information, and (ii) to test the ability of the constant capacitance model to predict B adsorption on additional soils. The B surface complexes used in the model application will be constrained to those observed in the spectroscopic study

---

USDA-ARS, U.S. Salinity Lab., 450 W. Big Springs Rd., Riverside, CA 92507. Contribution from the U.S. Salinity Lab. *Corresponding author (sgoldberg@ussl.ars.usda.gov).

Published in Soil Sci. Soc. Am. J. 63:823–829 (1999).

Abbreviations: ATR-FTIR, Attenuated Total Reflectance Fourier Transform Infrared; SA, surface area; suspension SD, suspension density.

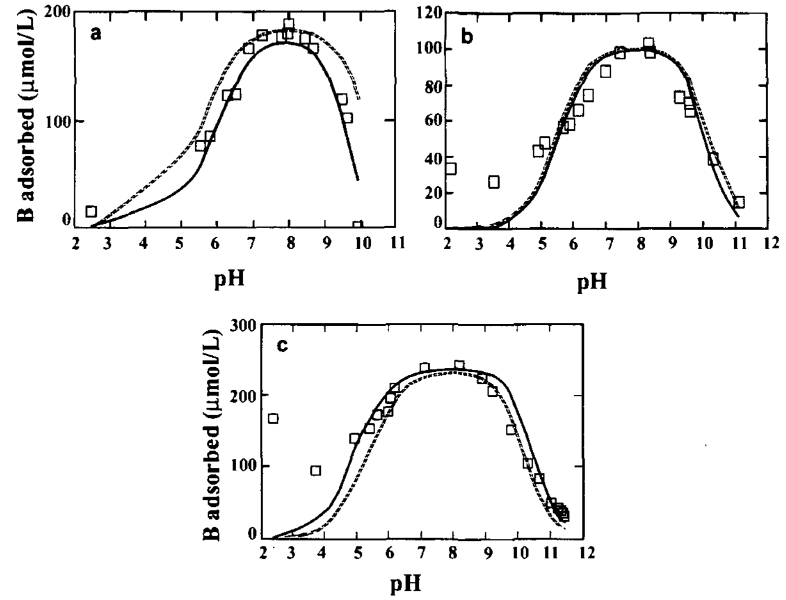

Fig. 1. Boron adsorption on Fe oxides: (a) hematite, suspension density (SD) = 100 g L^{-1}, surface area (SA) = 16.4 m^2 g^{-1}; (b) goethite, SD = 25 g L^{-1}, SA = 31.2 m^2 g^{-1}; and (c) amorphous Fe oxide, SD = 6.4 g L^{-1}, SA = 112 m^2 g^{-1}. Squares represent experimental data. Model fits are represented by solid lines. Model predictions are represented by dashed lines. Initial B concentration = 0.463 m*M*.

of Su and Suarez (1995). Inclusion of experimental spectroscopic observations into surface complexation models maximizes the chemical significance of model parameters. Identical surface complexation reactions will be used for all adsorbing materials. The ability of the constant capacitance model to predict B adsorption on additional soils using the fitted parameters obtained with the improved modeling approach will also be investigated. Predictive ability is an important criterion for incorporation of adsorption models into chemical speciation and transport models.

MATERIALS AND METHODS

Boron adsorption envelopes on oxides (Goldberg and Glaubig, 1985), clay minerals (Goldberg and Glaubig, 1986b), and soil samples (Goldberg and Glaubig, 1986a) were determined previously. Experimental methods and characterization of adsorbents are provided in these references. Physical and chemical characteristics and classifications of the soils are provided in Goldberg et al. (1988). The soil samples had the following range of characteristics: cation-exchange capacity: 29 to 229 mol_c L^{-1}, surface area: 28 to 196 m^2 g^{-1}, clay: 7 to 31% (smectite: 0.2–15%, kaolinite: 1–28%, illite 0.75–10%, vermiculite 0.1–3%), inorganic C: 0.001 to 1.9%, organic C: 0.12 to 0.89%, free Fe oxide: 0.27 to 1.7%, free Al oxide: 0.021 to 0.091%.

Boron adsorption isotherms were carried out on four additional soils using the procedure described by Goldberg and Glaubig (1985). Surface samples of the Porterville (fine, montmorillonitic, thermic Typic Chromoxerert), Wasco (coarse-loamy, mixed, nonacid, thermic Typic Torriorthent), Wyo (fine-loamy, mixed, thermic Mollic Haploxeralf), and Hesperia (coarse-loamy, mixed, nonacid, thermic Xeric Torriorthent)

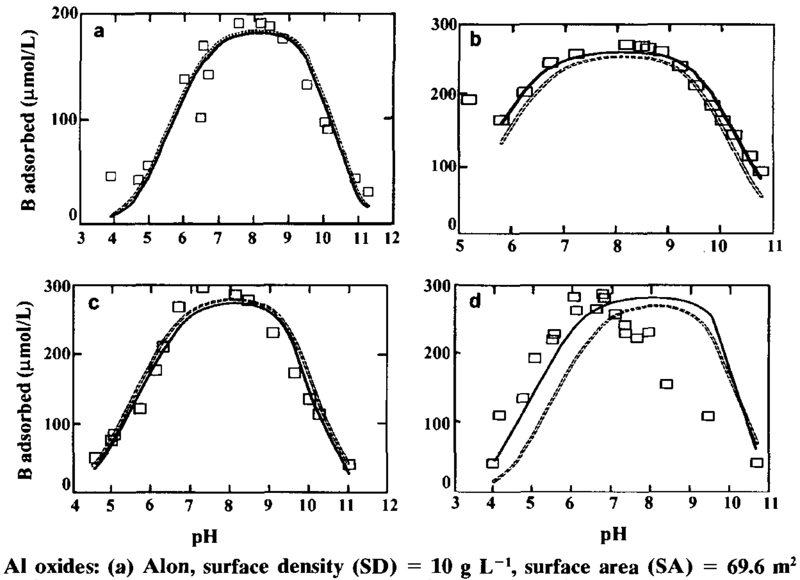

Fig. 2. Boron adsorption on Al oxides: (a) Alon, surface density (SD) = 10 g L^{-1}, surface area (SA) = 69.6 m^2 g^{-1}; (b) Aluminium Oxid C, SD = 40 g L^{-1}, SA = 96.9 m^2 g^{-1}; (c) pseudoboehmite, SD = 6.4 g L^{-1}, SA = 227 m^2 g^{-1}; (d) amorphous Al oxide, SD = 5.2 g L^{-1}, SA = 163 m^2 g^{-1}. Squares represent experimental data. Model fits are represented by solid lines. Model predictions are represented by dashed lines. Initial B concentration = 0.463 m*M*.

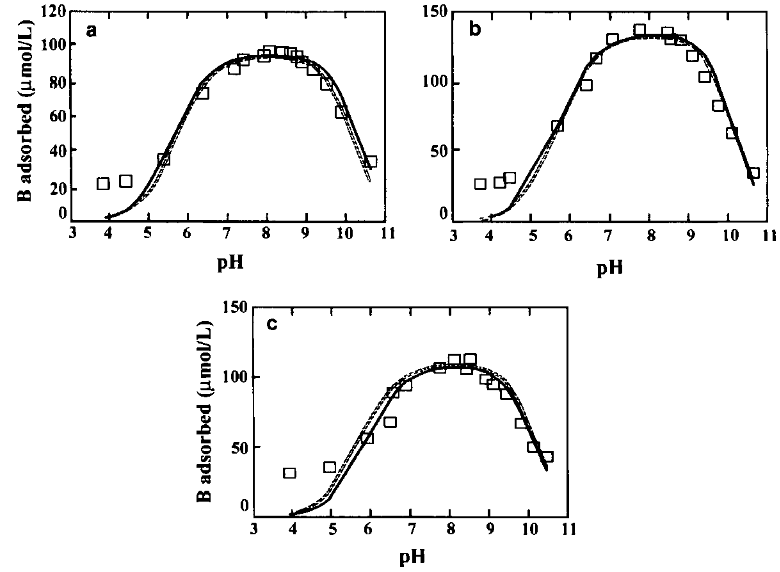

Fig. 3. Boron adsorption on kaolinites: (a) KGa-1 well crystallized kaolinite, SD = 200 g L^{-1}, SA = 8.1 m^2 g^{-1}; (b) KGa-2 poorly crystallized kaolinite, SD = 100 g L^{-1}, SA = 20.5 m^2 g^{-1}; (c) Georgia kaolinite, SD = 200 g L^{-1}, SA = 6.9 m^2 g^{-1}. Squares represent experimental data. Model fits are represented by solid lines. Model predictions are represented by dashed lines. Initial B concentration = 0.463 m*M*.

soil series consisted of the <2-mm fraction. The background electrolyte consisted of 0.1 *M* NaCl. Physical and chemical characteristics for these soils are provided in Goldberg et al. (1988). The ability of the constant capacitance model to predict B adsorption on these soils using average B surface complexation constants was evaluated. A detailed explanation of the theory and assumptions of the constant capacitance model is given in Goldberg (1992).

In the present application of the constant capacitance model to B adsorption, the following surface complexation reactions are included:

$$\mathrm{XOH} + \mathrm{H}^+ \rightleftharpoons \mathrm{XOH}_2^+ \qquad [1]$$

$$\mathrm{XOH} \rightleftharpoons \mathrm{XO}^- + \mathrm{H}^+ \qquad [2]$$

$$\mathrm{XOH} + \mathrm{B(OH)}_3 \rightleftharpoons \mathrm{XOB(OH)}_2 + \mathrm{H_2O} \qquad [3]$$

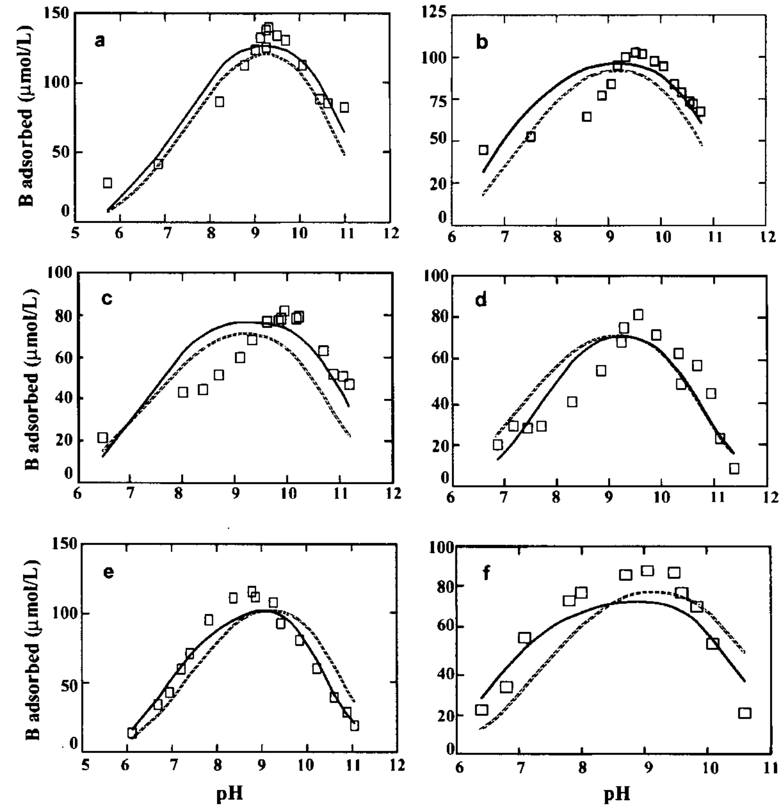

Fig. 4. Boron adsorption on 2:1 clays: (a) SAz-1 montmorillonite, SD = 40 g L^{-1}, SA = 18.6 m^2 g^{-1}; (b) STx-1 montmorillonite, SD = 40 g L^{-1}, SA = 53.6 m^2 g^{-1}; (c) SWy-1 montmorillonite, SD = 30 g L^{-1}, SA = 13.2 m^2 g^{-1}; (d) IMt-1 illite, SD = 50 g L^{-1}, SA = 11.8 m^2 g^{-1}, (e) Fithian illite, SD = 50 g L^{-1}, SA = 23.7 m^2 g^{-1}; (f) Morris illite, SD = 50 g L^{-1}, SA = 21.5 m^2 g^{-1}. Squares represent experimental data. Model fits are represented by solid lines. Model predictions are represented by dashed lines. Initial B concentration = 0.463 m*M*.

$$XOH + B(OH)_3 \rightleftharpoons XOB(OH)_3^- + H^+ \qquad [4]$$

where XOH represents the reactive-surface functional group: hydroxyls on oxides and aluminols on clay minerals and soils. Conventionally, reactions are written in terms of undissociated acids and neutral-surface sites. Alternative reactions starting with borate anion, $B(OH)_4^-$, and/or a positive surface site, XOH_2^+, could be written. Significant in this modeling approach is that the formation of both trigonal and tetrahedral B surface species is considered, consistent with the experimental spectroscopic results of Su and Suarez (1995).

Intrinsic equilibrium-constant expressions for the surface complexation reactions are:

$$K_+(\text{int}) = \frac{[XOH_2^+]}{[XOH][H^+]} \exp(F\psi/RT) \qquad [5]$$

$$K_-(\text{int}) = \frac{[XO^-][H^+]}{[XOH]} \exp(-F\psi/RT) \qquad [6]$$

$$K_B(\text{int}) = \frac{[XOB(OH)_2]}{[XOH][B(OH)_3]} \qquad [7]$$

$$K_{B^-}(\text{int}) = \frac{[XOB(OH)_3^-][H^+]}{[XOH][B(OH)_3]} \exp(-F\psi/RT) \qquad [8]$$

where F is the Faraday constant (C mol_c^{-1}), R is the molar gas constant (J mol^{-1} K^{-1}), T is the absolute temperature (K), and square brackets indicate concentrations (mol L^{-1}). The exponential terms can be considered solid phase activity coefficients that correct for the charges on the surface complexes.

Mass balance for the reactive surface functional group is:

$$[XOH]_T = [XOH] + [XOH_2^+] + [XO^-] + [XOB(OH)_2] + [XOB(OH)_3^-] \qquad [9]$$

Charge balance is:

$$\sigma = [XOH_2^+] - [XO^-] - [XOB(OH)_3^-] \qquad [10]$$

where σ has units of mol_c L^{-1}.

The computer program FITEQL 3.2 (Herbelin and Westall, 1996) was used to fit B surface complexation constants to the experimental data. FITEQL 3.2 uses a nonlinear least squares optimization technique to optimize equilibrium constants to experimental data. The FITEQL program contains the constant capacitance model of adsorption and can also be used as a chemical speciation model to evaluate predictions using previously determined equilibrium constants.

Input values for constant capacitance model parameters were the same as for the original applications (Goldberg and Glaubig, 1985 for oxides; Goldberg and Glaubig, 1986b for clays; Goldberg and Glaubig, 1986a for soils). The capacitance density was fixed at $C_d = 1.06$ F m^{-2}. The protonation constant, log K_+, and the dissociation constant, log K_-, were set at: log $K_+ = 7.31$, log $K_- = -8.80$ for Fe oxides and log $K_+ = 7.38$, log $K_- = -9.09$ for Al oxides and clays, and log $K_+ = 7.35$,

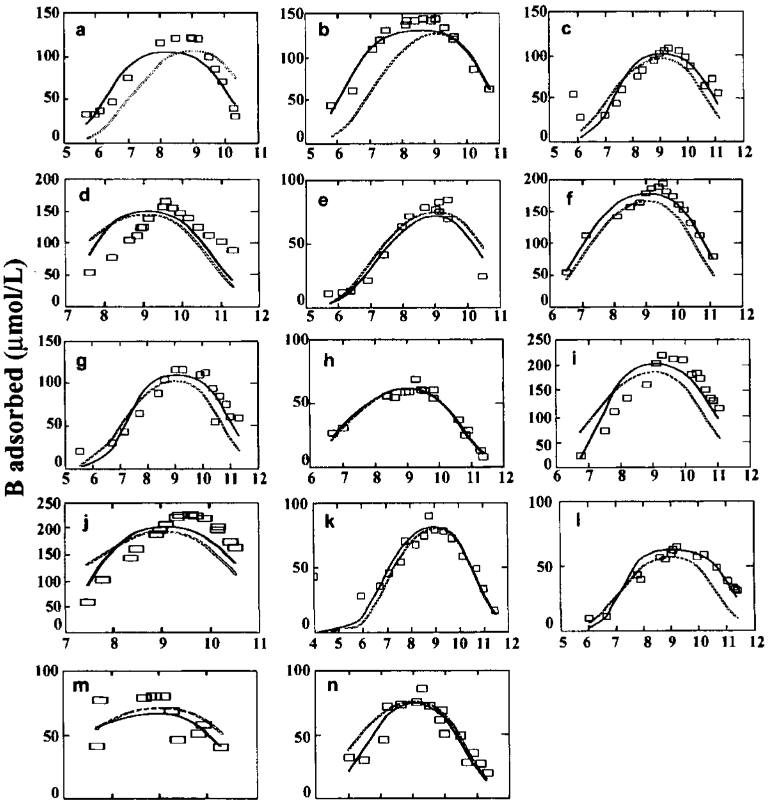

Fig. 5. Boron adsorption on soil samples: (a) Altamont soil, SA = 103 m^2 g^{-1}; (b) Altamont subsoil, SA = 114 m^2 g^{-1}; (c) Arlington soil, SA = 61.1 m^2 g^{-1}; (d) Arlington subsoil, SA = 103 m^2 g^{-1}; (e) Bonsall soil, SA = 32.9 m^2 g^{-1}; (f) Bonsall subsoil, SA = 106 m^2 g^{-1}; (g) Fallbrook soil, SA = 68.3 m^2 g^{-1}; (h) Fallbrook subsoil, SA = 28.5 m^2 g^{-1}; (i) Imperial soil, SA = 196 m^2 g^{-1}; (j) Imperial subsoil, SA = 191 m^2 g^{-1}; (k) Pachappa soil, SA = 36.3 m^2 g^{-1}; (l) Pachappa subsoil, SA = 41.0 m^2 g^{-1}; (m) Ramona soil, SA = 27.9 m^2 g^{-1}; (n) Ramona subsoil, SA = 38.8 m^2 g^{-1}. Squares represent experimental data. Model fits are represented by solid lines. Model predictions are represented by dashed lines. Suspension density = 200 g L^{-1}; initial B concentration = 0.463 m*M*.

log K_- = −8.95 for soils. The total number of reactive hydroxyl groups, $[XOH]_T$, was obtained experimentally from maximum B adsorption as was done in previous studies (Goldberg and Glaubig, 1985, 1986a, 1986b).

RESULTS AND DISCUSSION

Boron adsorption as a function of solution pH is indicated in the figures for Fe oxides (Fig. 1), Al oxides (Fig. 2), kaolinites (Fig. 3), 2:1 clay minerals (Fig. 4), and soils (Fig. 5 and 6). Boron adsorption increased with increasing solution pH until reaching a peak in adsorption, then decreased as solution pH was increased above the B adsorption maximum. The B adsorption maxima are located near pH 7 to 8 for oxides and kaolinites and in the pH range 9 to 10 for 2:1 clays and soils.

The fit of the constant capacitance model to B adsorption as a function of solution pH is indicated by a solid line in Fig. 1 for Fe oxides and Fig. 2 for Al oxides. With the exception of amorphous Al oxide, the model was well able to describe B adsorption on all materials. For amorphous Al oxide it was necessary to optimize the protonation–dissociation constants along with the B surface complexation constant to obtain a fit to the data. Values of the B surface complexation constants are provided in Table 1. Average values of log K_B and log K_{B-} are also provided in this table. Average values of the B surface complexation constants for both types of oxides are not statistically significantly different at the 95% level of confidence. The dashed lines in Fig. 1 and 2 indicate the model predictions for B adsorption using average sets of B surface complexation constants for Fe and Al oxides, respectively. Again, with the exception of amorphous Al oxide, the model predictions describe the adsorption data well. These results suggest that B surface complexation constants are not very different for various oxide minerals and that an average set of constants can probably be used to describe B adsorption behavior on other Fe and Al oxide minerals.

Surface pK_a values for adsorbed B can be calculated using the equilibrium constant values log K_B and log K_{B-} obtained with the constant capacitance model. For the surface reaction:

$$XOB(OH)_2 + H_2O \rightleftharpoons XOB(OH)_3^- + H^+ \quad [11]$$

the following pK_a values were obtained: 9.8 for goethite, 9.9 for amorphous Fe oxide, 9.7 for δ-Al_2O_3 (Alon, Cabot Corp., Boston, MA; Aluminium Oxid C, Degussa, Teterboro, NJ), and 9.9 for pseudoboehmite. These model-derived pK_a values compare favorably with the surface pK_a value of 8 to 9 for H_3BO_3 on amorphous Fe oxide postulated by Suarez et al. (1998) on

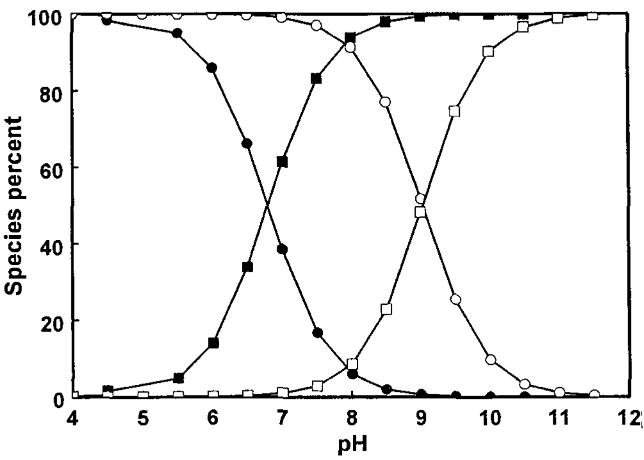

Fig. 6. Distribution of B surface species for two soil samples: (a) Pachappa subsoil (filled symbols), (b) Altamont soil (open symbols). Circles represent the distribution of $XOB(OH)_2$; squares represent the distribution of $XOB(OH)_3^-$.

Table 1. Surface complexation constants obtained with the constant capacitance model.

Solid	Log K_B(int)	Log K_{B-}(int)	Log K_+(int)†	Log K_-(int)‡	SOS/ DF§
		Fe oxides			
Hematite	4.71				88.9
Goethite	5.06	−4.72			116
Amorphous Fe oxide	5.63	−4.23			336
Average Fe oxides	5.13 ± 0.46	−4.48 ± 0.35			
		Al oxides			
Alon (δ-Al_2O_3)	4.94	−4.76			139
Aluminum Oxid C (δ-Al_2O_3)	5.22	−4.51			11.2
Pseudoboehmite	4.95	−4.98			54.7
Amorphous Al oxide	4.92		6.40	−7.45	143
Average Al oxides	5.01 ± 0.14	−4.75 ± 0.24			
		Kaolinites			
KGa-1 kaolinite	5.08	−4.69			35.4
KGa-2 kaolinite	5.07	−5.02			83.5
Georgia kaolinite	4.80	−4.88			69.7
Average kaolinites	4.98 ± 0.16	−4.86 ± 0.16			
		2:1 clays			
SAz-1 montmorillonite	3.55	−3.98			54.6
STx-1 montmorillonite	3.78	−3.95			50.6
SWy-1 montmorillonite	3.19	−3.82	9.23	−9.28	37.5
IMt-1 illite	2.92	−4.19			49.5
Fithian illite	3.66	−4.64			18.2
Morris illite	3.97	−4.49			48.8
Average 2:1 clays	3.51 ± 0.39	−4.17 ± 0.33			
		Soils			
Altamont soil	4.36	−4.67			57.0
Altamont subsoil	4.46	−4.16			24.8
Arlington soil	3.19	−3.84			56.4
Arlington subsoil		−4.67		−10.18	33.4
Bonsall soil	3.59	−4.35			32.4
Bonsall subsoil	3.89	−3.84			17.8
Fallbrook soil	3.38	−3.79			80.0
Fallbrook subsoil	3.80	−4.16			6.3
Imperial soil		−4.22	6.82	−9.60	24.9
Imperial subsoil		−4.34	7.29	−9.85	24.9
Pachappa soil	3.89	−4.10			90.7
Pachappa subsoil	3.23	−3.57			21.6
Ramona soil	3.86	−4.42			70.4
Ramona subsoil	3.23	−4.23			33.6
Average soils	3.72 ± 0.44	−4.17 ± 0.32			

† Unless indicated, Log K_+(int) was held constant at the value indicated in the text.

‡ Unless indicated, Log K_-(int) was held constant at the value indicated in the text.

§ A goodness-of-fit criterion that represents the overall variance in Y where SOS is the weighted sum of squares of the residuals and DF is the degrees of freedom. The smallest numbers for SOS/DF indicate the best fit.

the basis of analysis of the ATR-FTIR spectra obtained by Su and Suarez (1995). The model-derived pK_a values are slightly higher than the pK_a value for H_3BO_3 in aqueous solution (9.2), suggesting a somewhat greater proportion of $B(OH)_3$ on the surface than predicted from its speciation in solution.

The fits obtained with the constant capacitance model (Fig. 1 and 2) are very similar in quality to those obtained by Goldberg and Glaubig (1985, see Fig. 2 and 1, respectively) optimizing only the B surface complex, $XOB(OH)_2$. Since the model predicts $XOB(OH)_2$ to be the dominant B surface species until pH 9.7, addition of the surface species $XOB(OH)_3^-$ provides only a slight improvement in fit. Nonetheless, the present modeling approach is considered superior since the B surface species postulated are consistent with experimental spectroscopic observations. Because values of the protonation and dissociation constants were also used as adjustable parameters in the earlier study, the fit of the model to B adsorption on amorphous Al oxide presented by Goldberg and Glaubig (1985, Fig. 1d) describes the data more closely than the present model fit (Fig. 2d).

Figure 3 presents the fit of the constant capacitance model to B adsorption on three kaolinite clays. The model describes the data very well on all three materials. As expected when increasing the number of adjustable parameters, the fits in Fig. 3, using both $XOB(OH)_2$ and $XOB(OH)_3^-$, are improved over those presented by Goldberg and Glaubig (1986b, Fig. 1) using $XOB(OH)_2$. Values of the B surface complexation constants and average values of log K_B and log K_{B-} for kaolinites are presented in Table 1. Average values of the B surface complexation constants for kaolinites are not statistically significantly different from those for Al and Fe oxides at the 95% level of confidence. Dashed lines in Fig. 3 indicate the model predictions of B adsorption obtained using an average set of B surface complexation constants for kaolinites. The model predictions describe the B adsorption data equally well as the model fits, indicating that the average set of surface complexation constants can be used to describe B adsorption behavior on other kaolinite minerals. Surface pK_a values for reaction [11] are: 9.8 for well crystallized kaolinite, 10.1 for poorly crystallized kaolinite, and 9.7 for Georgia kaolinite. These values are comparable in magnitude to those for Al and Fe oxides, reflecting the similarity in values of the B surface complexation constants of all of these materials.

The ability of the constant capacitance model to describe B adsorption on the 2:1 clay minerals, montmorillonite and illite, is presented in Fig. 4. Overall, the model was able to describe B adsorption on 2:1 minerals, fitting a smooth curve through the data. The shape of the model fit is parabolic in nature, leading to some underprediction of the data near the pointed adsorption maxima. For SWy-1 montmorillonite it was necessary to optimize the protonation–dissociation constants along with the B surface complexation constant to obtain a fit to the data. Values of the B surface complexation constants and average values of log K_B and log K_{B-} for 2:1 clays are provided in Table 1. Average values of the B surface complexation constants for 2:1 clays are statistically significantly different from those for kaolinites at the 95% level of confidence. Model predictions using the average set of B surface complexation constants are indicated in Fig. 4 by dashed lines. The model predictions represent the data less closely than the model fits but provide an adequate description. These results suggest some predictive utility of average sets of B surface complexation constants for describing B adsorption behavior on additional 2:1 clay minerals.

The model fits presented in Fig. 4 are approximately similar in quality to those obtained by Goldberg and Glaubig (1986b, Fig. 2 and 3). It is significant to note that the model fits in the present study were obtained by optimizing constants for two B surface species — $XOB(OH)_2$ and $XOB(OH)_3^-$ –, while the model fits of

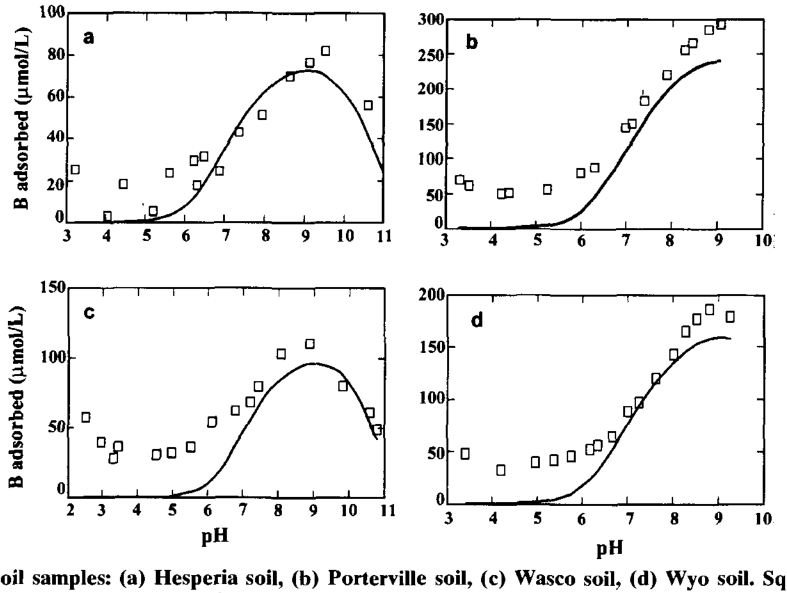

Fig. 7. Boron adsorption on soil samples: (a) Hesperia soil, (b) Porterville soil, (c) Wasco soil, (d) Wyo soil. Squares represent experimental data. Model predictions are represented by solid lines. Initial B concentration = 0.463 m*M*.

Goldberg and Glaubig (1986b) were obtained by optimizing three constants, $XOB(OH)_2$ for the B surface species and values for the protonation constant log K_+, and the dissociation constant log K_-. In the optimization process, Goldberg and Glaubig (1986b) obtained unrealistic values of log K_+ and log K_- for one montmorillonite and one illite. The present modeling approach is considered superior because: (i) one less adjustable parameter is optimized; (ii) identical values of log K_+ and log K_- are used for all 2:1 clays; (iii) unrealistic values of log K_+ and log K_- are avoided. Surface pK_a values for adsorbed B are: 7.5 for SAz-1 montmorillonite, 7.4 for STx-1 montmorillonite, 7.0 for SWy-1 montmorillonite, 7.1 for IMt-1 illite, 8.3 for Fithian illite, and 8.5 for Morris illite. These pK_a values are significantly lower than those for Al and Fe oxides and kaolinite clays, suggesting a much greater role for the surface species $XOB(OH)_3^-$ in B adsorption on 2:1 clays.

The ability of the constant capacitance model to describe B adsorption as a function of solution pH on 14 arid-zone soil samples is indicated in Fig. 5. The model provides a quantitative description of B adsorption behavior on all soils except for Altamont soil and subsoil, Arlington subsoil, and Imperial subsoil. For these samples, the model describes the data qualitatively. For Arlington subsoil, and Imperial soil and subsoil it was necessary to optimize the protonation–dissociation constants along with the B surface complexation constant to obtain a fit to the data; for these soils log K_B(int) did not converge. Table 1 provides values of the B surface complexation constants and average values of log K_B and log K_{B-} for soils. Average values of the B surface complexation constants for soils are not statistically significantly different from those of 2:1 clays at the 95% level of confidence. This result is consistent with the fact that clay minerals are important B-adsorbing sites in arid-zone soils (Elrashidi and O'Connor, 1982).

The model fits obtained in Fig. 5 are comparable with those obtained for these soils by Goldberg and Glaubig (1986a). As for the 2:1 clay minerals, it is significant to note that the present model fits were obtained by optimizing two surface constants (K_B and K_{B-}), while the model fits of Goldberg and Glaubig (1986a) were obtained by optimizing three surface constants (K_B, K_+, and K_-). In carrying out their optimization, Goldberg and Glaubig (1986a) obtained unrealistic values of log K_+ for one soil and of log K_- for five soils. As for 2:1 clays, the modeling approach of the present study is considered superior because one less parameter is adjusted and identical log K_+ and log K_- values are used for all soils, thus avoiding unrealistic values of these parameters. Surface pK_a values for adsorbed B range from 6.8 for Pachappa subsoil to 9.0 for Altamont soil. The distribution of B surface species for these two soils are presented in Fig. 6. For the Pachappa subsoil the $XOB(OH)_3^-$ species dominates across most of the pH range, while for the Altamont soil $XOB(OH)_2$ is dominant across most of the pH range.

Dashed lines in Fig. 5 indicate model predictions of B adsorption obtained using an average set of B complexation constants for soils. The model predictions represent the data slightly less closely than the model fits but still provide a reasonable description. The ability of the average set of B surface complexation constants to predict B adsorption behavior was tested on four additional arid-zone soils and is presented in Fig. 7. The model was able to predict B adsorption behavior on all four soils, fitting a smooth parabolic curve through the data. These results indicate the utility of the average set of B surface complexation constants for predicting B adsorption on other arid-zone soils. The capability of these constants to describe B adsorption on soils of higher oxide and organic matter content remains to be evaluated.

Incorporation of microscopic experimental information into the macroscopic constant capacitance model improves its ability to describe B adsorption data. Boron adsorption on a variety of surfaces was described using one set of model reactions. The set of model parameters determined in this investigation can be used to predict B adsorption on other arid-zone soil samples.

REFERENCES

Adriano, D.C. 1986. Trace elements in the terrestrial environment. Springer-Verlag, New York.

Bloesch, P.M., L.C. Bell, and J.D. Hughes. 1987. Adsorption and desorption of boron by goethite. Aust. J. Soil Res. 25:377–390.

Elrashidi, M.A., and G.A. O'Connor. 1982. Boron sorption and desorption in soils. Soil Sci. Soc. Am. J. 46:27–31.

Goldberg, S. 1992. Use of surface complexation models in soil chemical systems. Adv. Agron. 47:233–329.

Goldberg, S., and H.S. Forster. 1991. Boron sorption on calcareous soils and reference calcites. Soil Sci. 152:304–310.

Goldberg, S., and R.A. Glaubig. 1985. Boron adsorption on aluminum and iron oxide minerals. Soil Sci. Soc. Am. J. 49:1374–1379.

Goldberg, S., and R.A. Glaubig. 1986a. Boron adsorption on California soils. Soil Sci. Soc. Am. J. 50:1173–1176.

Goldberg, S., and R.A. Glaubig. 1986b. Boron adsorption and silicon release by the clay minerals kaolinite, montmorillonite, and illite. Soil Sci. Soc. Am. J. 50:1442–1448.

Goldberg, S., D.L. Suarez, and R.A. Glaubig. 1988. Factors affecting clay dispersion and aggregate stability of arid zone soils. Soil Sci. 146:317–325.

Herbelin, A.L., and J.C. Westall. 1996. FITEQL: A computer program for determination of chemical equilibrium constants from experimental data. Rep. 94-01, Version 3.2, Dep. of Chemistry, Oregon State Univ., Corvallis.

Reisenauer, H.M., L.M. Walsh, and R.G. Hoeft. 1973. Testing soils for sulphur, boron, molybdenum, and chlorine. p. 173–200. *In* L.M. Walsh and J.D. Beaton (ed.) Soil testing and plant analysis. rev. ed. SSSA, Madison, WI.

Singh, P.N., and S.V. Mattigod. 1992. Modeling boron adsorption on kaolinite. Clays Clay Miner. 40:192–205.

Sposito, G. 1983. Surface complexation model of the oxide-aqueous solution interface. J. Colloid Interface Sci. 91:329–340.

Stumm, W., R. Kummert, and L. Sigg. 1980. A ligand exchange model for the adsorption of inorganic and organic ligands at hydrous oxide interfaces. Croatica Chem. Acta 53:291–312.

Su, C., and D.L. Suarez. 1995. Coordination of adsorbed boron: A FTIR spectroscopic study. Environ. Sci. Technol. 29:302–311.

Suarez, D.L., S. Goldberg, and C. Su. 1998. Evaluation of oxyanion adsorption mechanisms on oxides using FTIR spectroscopy and electrophoretic mobility. *In* D.L. Sparks and T. Grundl (ed.) Kinetics and mechanisms of reactions at the mineral/water interface. Am. Chem. Soc. Symp. Ser. 715:136–178.

Toner, C.V., and D.L. Sparks. 1995. Chemical relaxation and double layer model analysis of boron adsorption on alumina. Soil Sci. Soc. Am. J. 59:395–404.